JCB Report

RanGAP1*SUMO1 is phosphorylated at the onset of mitosis and remains associated with RanBP2 upon NPC disassembly

Sowmya Swaminathan, Florian Kiendl, Roman Körner, Raffaella Lupetti, Ludger Hengst, and Frauke Melchior

Max-Planck Institute for Biochemistry, 82152 Martinsried, Germany

The RanGTPase activating protein RanGAP1 has essential functions in both nucleocytoplasmic transport and mitosis. In interphase, a significant fraction of vertebrate SUMO1-modified RanGAP1 forms a stable complex with the nucleoporin RanBP2/Nup358 at nuclear pore complexes. RanBP2 not only acts in the RanGTPase cycle but also is a SUMO1 E3 ligase. Here, we show that RanGAP1 is phosphorylated on residues T409, S428, and S442. Phosphorylation occurs before nuclear envelope breakdown and is maintained throughout mitosis. Nocodazole arrest leads to quantitative phosphorylation. The M-phase kinase cyclin B/Cdk1 phosphorylates RanGAP1 efficiently in vitro, and T409 phosphorylation correlates with nuclear accumulation of cyclin B1 in vivo. We find that phosphorylated RanGAP1 remains associated with RanBP2/Nup358 and the SUMO E2–conjugating enzyme Ubc9 in mitosis, hence mitotic phosphorylation may have functional consequences for the RanGTPase cycle and/or for RanBP2-dependent sumoylation.

Introduction

The GTPase Ran serves essential roles in nucleocytoplasmic transport, mitotic spindle formation, checkpoint control, and postmitotic nuclear envelope reassembly (Arnaoutov and Dasso, 2003; Quimby and Dasso, 2003; Walther et al., 2003). These functions are accomplished in part by the asymmetric localization of the RanGTPase activating protein RanGAP1 and the guanine-nucleotide exchange factor RCC1. RCC1 is dynamically chromatin associated in interphase and mitosis (Li et al., 2003). RanGAP1 is cytoplasmic in interphase cells, with a large fraction stably associated with the nucleoporin RanBP2/Nup358 at the cytoplasmic face of the nuclear pore complex (NPC). This interaction requires modification of RanGAP1 with the ubiquitin-related protein SUMO1 (Matunis et al., 1996; Mahajan et al., 1997). Interestingly, RanBP2 serves both as a docking factor in transport and as an E3 ligase for sumoylation (Pichler et al., 2002). In mitosis, RanGAP1 and RanBP2 are diffusely distributed throughout the cell, albeit a small fraction of both proteins is also observed at the mitotic spindle and at kinetochores (Matunis et al., 1996; Joseph et al., 2002).

To accommodate Ran's different functions in interphase and mitosis, components of the RanGTPase cycle are likely to be cell cycle regulated. A first example is the RanGTP interacting protein RanBP1, whose levels increase from S-phase to metaphase and decline during late telophase (Guarguaglini et al., 2000). RanBP2 is hyperphosphorylated during mitosis, but the consequences of this are unknown (Favreau et al., 1996). Here, we show that RanGAP1 is subject to mitotic phosphorylation at three closely spaced residues in its COOH-terminal domain. Phosphorylation occurs at the NPC before nuclear envelope breakdown, but does not disrupt the RanGAP1*SUMO1–RanBP2–Ubc9 interaction. RanGAP1 phosphorylation may potentially alter RanGAP1's catalytic activity or RanBP2-mediated sumoylation in vivo.

Results and discussion

RanGAP1 is phosphorylated during mitosis

To investigate whether or not RanGAP1 undergoes cell cycle–dependent changes, we synchronized HeLa cells in early S-phase and took samples as cells progressed through the cell cycle. Immunoblotting revealed that RanGAP1

The online version of this article includes supplemental material.

Address correspondence to F. Melchior, Max-Planck Institute for Biochemistry, Am Klopferspitz 18, D-82152 Martinsried, Germany. Tel.: (49) 89 8578 3972. Fax: (49) 89 8578 3810.
email: melchior@biochem.mpg.de

S. Swaminathan's present address is Nature Cell Biology, The Macmillan Building, 4 Crinan Street, London N19XW, UK.

Key words: RanGAP1; RanBP2/Nup358; SUMO; cyclin B/Cdk1; Ubc9

Abbreviations used in this paper: MALDI-TOF, matrix-assisted laser desorption/ionization time-of-flight; NPC, nuclear pore complex.

The Journal of Cell Biology, Volume 164, Number 7, March 29, 2004 965–971
http://www.jcb.org/cgi/doi/10.1083/jcb.200309126

The Journal of Cell Biology

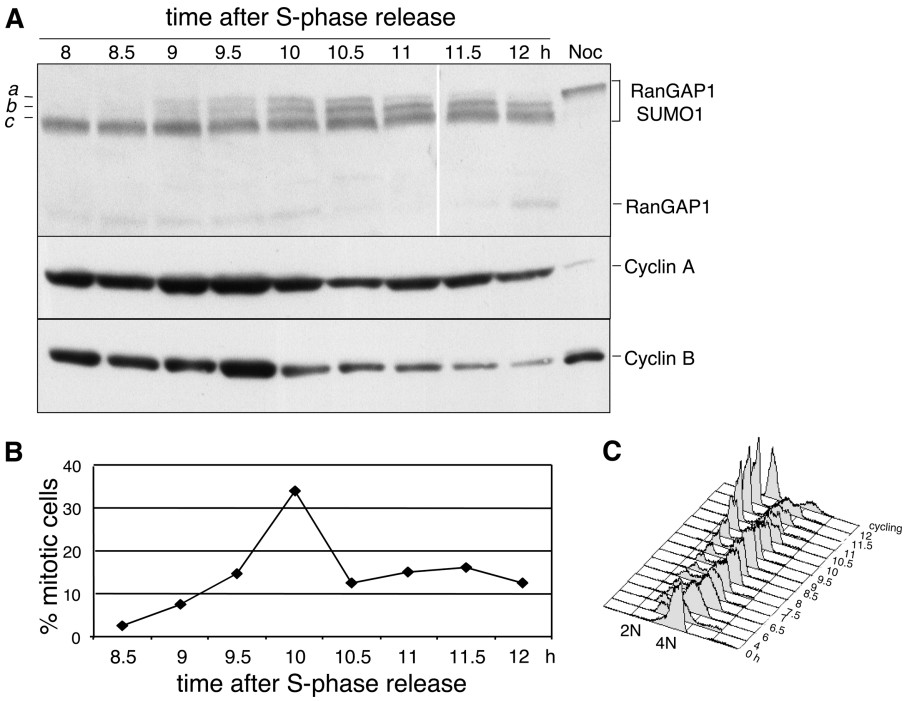

Figure 1. **Cell cycle–dependent phosphorylation of RanGAP1.** (A) HeLa cells arrested in S-phase with thymidine were released from the S-phase block, harvested at the indicated times, and analyzed by immunoblotting with antibodies to RanGAP1, cyclin A, and cyclin B. For optimal resolution of RanGAP1 species a, b, and c, 6% SDS-PAGE was used for the top panel. Note that all time points were run on the same gel. (B) Mitotic index was determined by visually scoring fixed cells stained with Hoechst for the presence of condensed chromosomes. About 200 cells were scored at each time point. (C) Cell cycle analysis: DNA content of each sample was determined by propidium iodine staining and analysis by flow cytometry.

abundance and sumoylation level remained unchanged (Fig. 1 A). However, two species of SUMO1-modified RanGAP1 with lower mobility (Fig. 1 A, bands a and b) were first visible at a time coincident with the onset of mitosis (9 h after release). Maximal levels of these species were observed at 10 h after release, at which time the mitotic index was highest (34%). Cyclin A and B1 protein levels had already declined, indicating that the majority of cells had progressed through the metaphase–anaphase transition at this point. Nocodazole arrest led to quantitative conversion of sumoylated RanGAP1 into the species designated band a (Fig. 1 A). Phosphatase treatment demonstrated that bands a and b represent phosphorylated RanGAP1 (unpublished data).

Identification of three phosphorylation sites in RanGAP1

Mass spectrometry was used to identify the phosphorylated residues in RanGAP1 (Fig. 2). For this process, species represented by bands a, b, and c were enriched by immunoprecipitation from nocodazole and interphase lysates (Fig. 2 A). Bands a and c were obtained from digitonin-lysates, band b was obtained from hypotonic swelling lysates (for unknown reasons, band a was rapidly converted to band b during hypotonic swelling). Coomassie-stained bands a, b, and c were subjected to in-gel digestion by trypsin and analyzed by matrix-assisted laser desorption/ionization time-of-flight (MALDI-TOF) mass spectrometry (Fig. 2 B). A peptide (amino acids 407–445 in human RanGAP1) containing up to three phosphates was identified; only the unphosphorylated species was obtained from band c, up to two phosphates were detected in the peptide from band b, and two or three phosphates were present in the peptide from band a. From this analysis, we concluded that the two RanGAP1 phosphoforms a and b were phosphorylated at three and two residues, respectively. The two phosphorylated residues in band b were unequivocally identified as Ser 428 and Ser 442 through sequencing of the doubly phosphorylated peptide 414–445 by electrospray ionization ion trap mass spectrometry (Fig. 2 C).

Identification of the three sites in band a failed with this method. We considered it likely that band a was also phosphorylated at Ser 428 and Ser 442. A good candidate for the third residue was Thr 409, as it is part of a consensus motif for Cdks (TPSRK). To test if Thr 409 was phosphorylated in vivo, and to confirm phosphorylation at the other sites, we generated three phosphospecific antibodies directed toward p-T409, p-S428, and p-S442. These antibodies were used to probe RanGAP1 immunoprecipitated from interphase and nocodazole extracts (Fig. 2 D). Indeed, mitotic phosphorylation of RanGAP1 occurs at T409, S428 and S442. Band a is phosphorylated at all three residues, whereas band b is only phosphorylated at S428 and S442.

Phosphorylation of RanGAP1 occurs before nuclear envelope breakdown

Next, we tested the phosphospecific antibodies in immunofluorescence. α p-T409 strongly decorates cells from prophase to telophase. Fig. 3 A shows representative images for different mitotic stages. In metaphase and anaphase, strong cytoplasmic staining and some enhancement at the mitotic spindle was visible, consistent with previous reports on RanGAP1 localization in mitosis (Matunis et al., 1996; Joseph et al., 2002). α P-S428 and α P-S442 antibodies are weaker and appear to give rise to more background, but they also clearly decorate mitotic cells (Fig. 3 B). Interestingly, relative intensities of signals between prophase and telophase varied for the three antibodies, suggesting differential timing of phosphorylation or dephosphorylation. To address this issue, we immunoprecipitated RanGAP1 from cells at different time points after thymidine release and detected RanGAP1 by immunoblotting with the phosphospecific antibodies (Fig. 3 C). At 9 h after release, band a is already

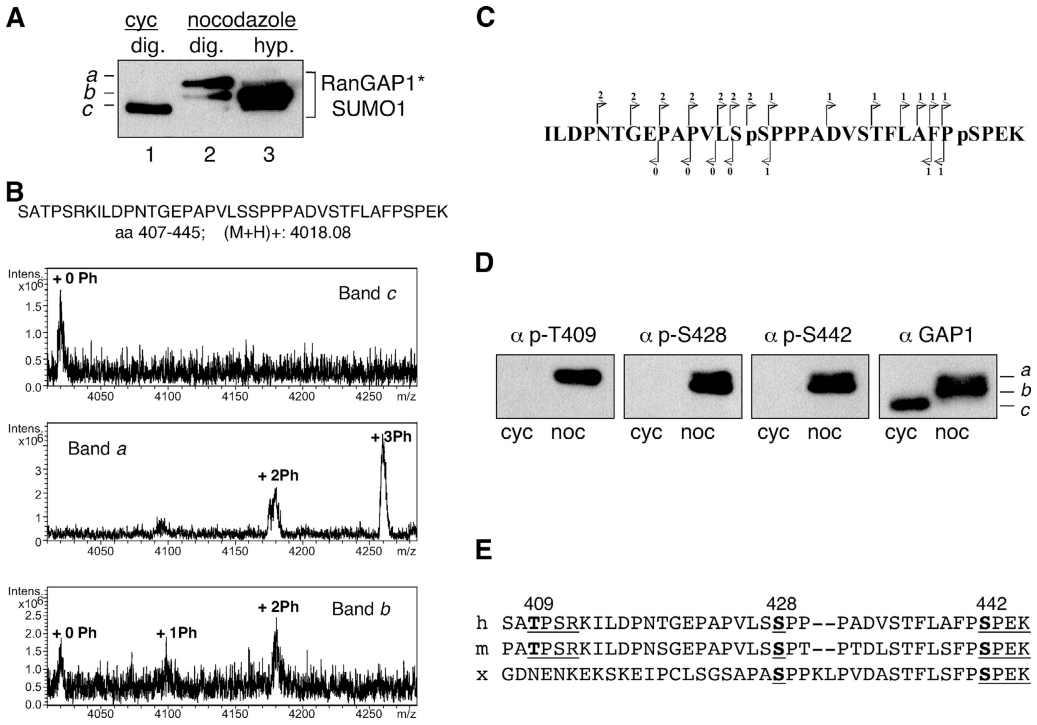

Figure 2. **Mitotic RanGAP1 is phosphorylated at residues T409, S428, and S442 in vivo.** (A) RanGAP1 species required for mass spectrometry (indicated as bands a, b, and c) were enriched by immunoprecipitation from HeLa cell extracts. A fraction of the precipitates was subjected to immunoblotting with α-RanGAP1 antibodies. The remainder was separated on SDS-PAGE (not depicted), and Coomassie-stained bands a, b, and c were excised from lanes 2, 3, and 1, respectively. cyc, cycling cells; nocodazole, nocodazole-arrested cells; dig, digitonin lysis; hyp, hypotonic swelling extracts. (B) MALDI-TOF mass spectra of a tryptic digest of RanGAP1 species enriched as described in A. Top, band c; middle, band a; bottom, band b. A peptide (amino acids 407–445 in human RanGAP1) containing up to three phosphates was identified. A selected mass range containing different phosphorylation stages (0, 1, 2, and 3 Ph) of this peptide is depicted. (C) Scheme showing the localization of two phosphorylation sites through fragmentation of the doubly phosphorylated peptide (amino acids 414–445) of RanGAP1 using an electrospray ionization ion trap mass spectrometer. The number of phosphorylation sites that were observed on each fragment is added as an arabic number to the arrows. (D) RanGAP1 immunoprecipitated with α RanGAP1 antibodies from cycling and nocodazole-arrested HeLa cells was analyzed by immunoblotting with the indicated phosphospecific antibodies. (E) All three phosphorylation sites of human RanGAP1 are conserved in mouse, areas surrounding S442 and S428 are also conserved in *Xenopus laevis* RanGAP1.

present, whereas little singly phosphorylated S442 (comigrating with unphosphorylated RanGAP1) and no singly phosphorylated T409 or S428 is detectable. This finding suggests that RanGAP1 is initially phosphorylated at all three sites. In contrast, dephosphorylation appears sequential, as p-T409 clearly disappears before the other two phosphorylated sites. Together, we find that RanGAP1 is phosphorylated at the onset of mitosis before nuclear envelope breakdown. Differential timing of dephosphorylation of the three sites in RanGAP1 results in at least three distinct mitotic RanGAP1 species: a triply phosphorylated species, and two species phosphorylated at both S428 and S442 or only at S442.

Cdks phosphorylate RanGAP1

Threonine 409 and serine 442 in human RanGAP1 (T411 and S444 in murine RanGAP1; Fig. 2 E) lie within consensus motifs for Cdks (T/S-P-X-K/R; Kreegipuu et al., 1999). Therefore, we tested whether or not Cdks present in nocodazole extracts contribute to RanGAP1 phosphorylation. In vitro sumoylated RanGAP1 was incubated with nocodazole extracts in the presence or absence of the Cdk-specific inhibitor p27 (Hengst and Reed, 1998). Indeed, incubation with p27 prevented the appearance of a higher molecular weight form (Fig. 4 A), indicating that Cdk activity was indeed required for RanGAP1 phosphorylation. Next, we demonstrated efficient in vitro phosphorylation of RanGAP1 with two recombinant Cdks, cyclin A/Cdk2 and cyclin B/Cdk1(Fig. 4 B). Mutagenesis of Thr 411, but not of Ser 444, severely reduced phosphorylation by either kinase, and phosphorylation was completely abolished in the double mutant T411D, S444D (Fig. 4 B). These data demonstrate that recombinant cyclin A/Cdk2 and cyclin B/Cdk1 phosphorylate mouse RanGAP1 in vitro, with a strong preference for Thr 411. Considering the timing and location of RanGAP1 phosphorylation, Cdk1, but not the G1/S kinase Cdk2, is a likely candidate in vivo. Three major Cdk1 kinases contribute to mitosis, cyclin A/Cdk1, cyclin B1/Cdk1, and cyclin B2/Cdk1. Of these, cyclin B1/Cdk1 is the most obvious candidate. Cyclin B1, which is already expressed in the G2 phase of the cell cycle, forms a complex with inactive Cdk1 and is localized in the cytoplasm. At the onset of mitosis, cyclin B1/Cdk1 rapidly accumulates in the nucleus (Yang and Kornbluth, 1999; Takizawa and Morgan, 2000; Toyoshima-Morimoto et al., 2001). Double labeling with α cyclin B1 and α p-T409 antibodies (Fig. 4 C) demonstrated that strong nuclear envelope

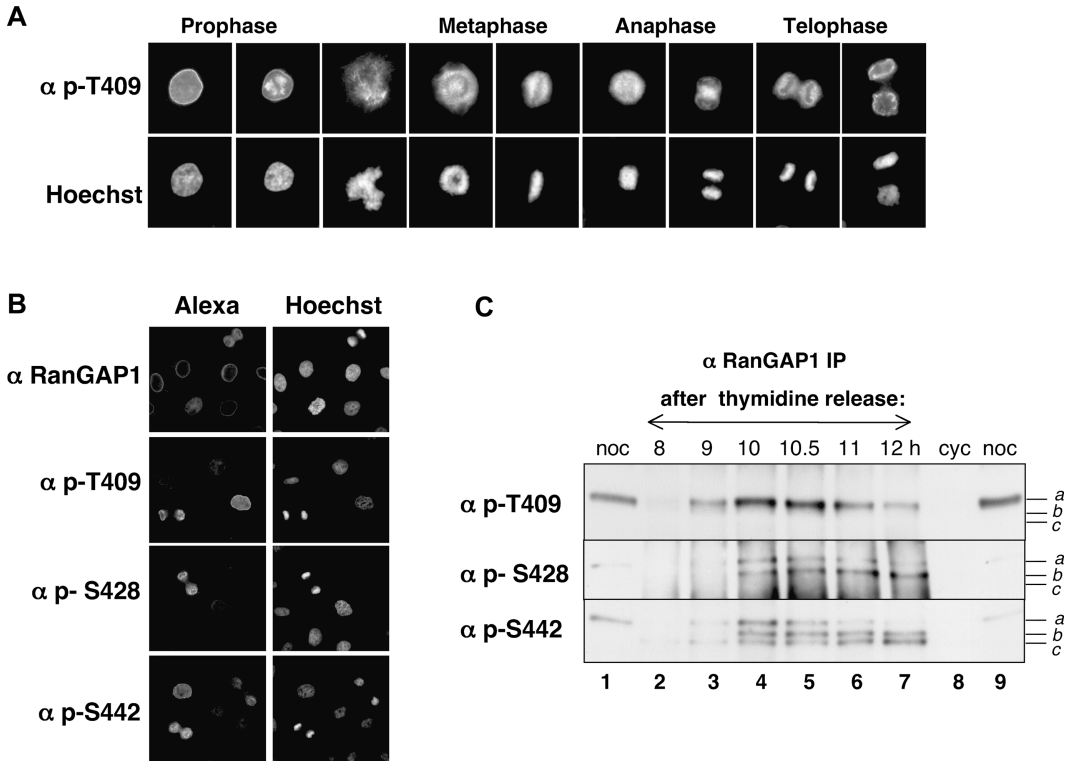

Figure 3. **RanGAP1 phosphorylation takes place before nuclear envelope breakdown.** (A) HeLa cells fixed and permeabilized with 4% PFA and 0.2% Triton X-100 were subjected to indirect immunofluorescence with α p-T409 antibody. (B) HeLa cells were fixed with 2% PFA, permeabilized with 0.2% Triton X-100, and stained with primary antibodies as indicated. (C) At least three distinct phosphorylated RanGAP1 species exist during mitosis. (lanes 2–7) α RanGAP1 immunoprecipitates from cells harvested at indicated times after release from thymidine (same cells as in Fig. 1). (lanes 1, 8, and 9) Total extracts from cycling (cyc) and nocodazole (noc) extracts served as controls. Immunoblotting was done with the indicated phosphospecific antibodies.

labeling was first seen in prophase cells with intranuclear cyclin B1 and condensed chromatin (Fig. 4 C). Collectively, these findings make cyclin B1/Cdk1 the best candidate for phosphorylating T409.

RanGAP1 phosphorylation does not disrupt interactions with RanBP2 and Ubc9

Mitotic phosphorylation by cyclin B/Cdk1 has been suggested to facilitate disassembly and, potentially, reassembly

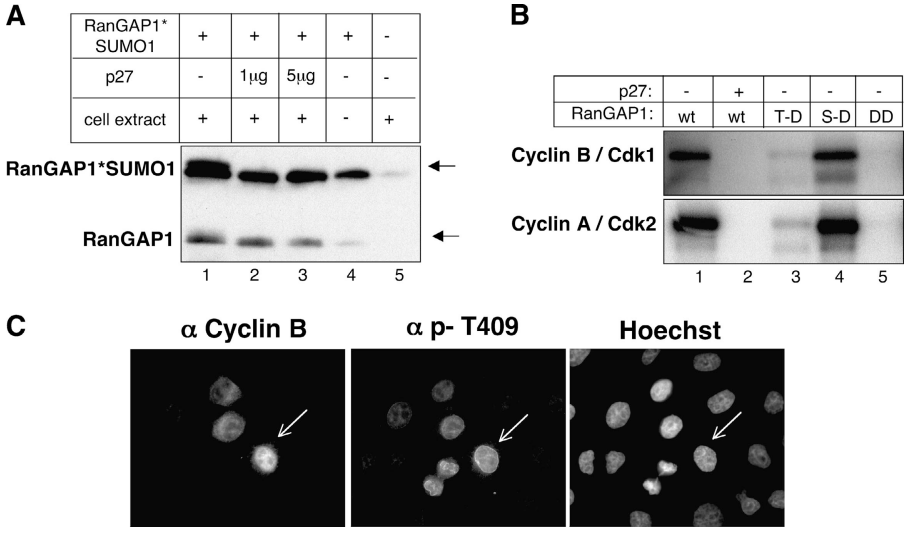

Figure 4. **RanGAP1 phosphorylation by Cdks.** (A) Phosphorylation of RanGAP1 in HeLa cell extracts is inhibited by p27. Recombinant sumoylated RanGAP1 was incubated with nocodazole extracts in the presence of ATP and analyzed by immunoblotting with α RanGAP1. Phosphorylation results in a mobility shift (arrows). Where indicated, extracts were preincubated with p27 before RanGAP1*SUMO1 addition. (B) In vitro phosphorylation of recombinant RanGAP1 with cyclin A/Cdk2 or cyclin B/Cdk1. After incubation, samples were analyzed by SDS-PAGE and autoradiography. p27 was included to demonstrate specificity of the kinase preparations. Mouse RanGAP1 mutants: T-D, RanGAP1-T411D; S-D, RanGAP1-S444D; DD, RanGAP1-T411D, S444D. (C) In vivo phosphorylation of human RanGAP1 T409 correlates with levels and localization of cyclin B. HeLa cells fixed with 2% PFA and permeabilized with 0.2% Triton X-100 were stained with α p-T409 antibodies and α cyclin B.

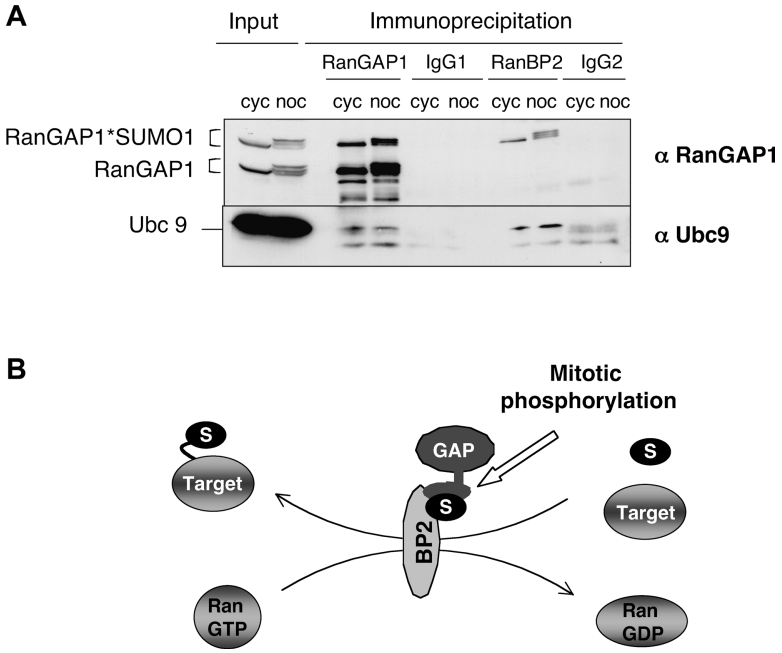

Figure 5. **RanGAP1*SUMO1 phosphoforms a and b remain associated with RanBP2 and Ubc9 in nocodazole-arrested HeLa cells.** (A) α RanGAP1 and α RanBP2 immunoprecipitates from cycling and nocodazole-arrested cells (RIPA extracts) were analyzed for the presence of RanGAP1 (top) and Ubc9 (bottom) by immunoblotting. IgGs 1 and 2 were from the respective preimmune sera and served as specificity controls. (B) Model: the RanGAP1*SUMO1–RanBP2 complex serves a dual function as an activator of Ran-GTP hydrolysis and as a SUMO E3 ligase. Either process may be affected by mitotic phosphorylation of RanGAP1.

of NPCs (Macaulay et al., 1995; Favreau et al., 1996). RanGAP1 phosphorylation at the G2–M transition takes place at residues directly adjacent to and within the domain required for interaction with RanBP2 (amino acids 420–470 in mouse RanGAP1; Matunis et al., 1998). Therefore, it was possible that phosphorylation disrupts this interaction as part of the NPC disassembly process. However, as shown in Fig. 5 A (top), phosphorylated RanGAP1 coimmunoprecipitated with RanBP2 from RIPA buffer extracts, indicating that the RanGAP1*SUMO1–RanBP2 complex is maintained stably in mitosis. It has previously been shown that a small fraction of the SUMO E2 enzyme Ubc9 is associated with the RanGAP1*SUMO1–RanBP2 complex at the NPC in interphase (Zhang et al., 2002). As shown in Fig. 5 A, Ubc9 also coimmunoprecipates with RanGAP1 and RanBP2 from mitotic extracts (bottom).

Possible functions of RanGAP1 phosphorylation

We find that sumoylated RanGAP1 remains associated with RanBP2 and Ubc9 in mitosis, irrespective of its phosphorylation state. This complex regulates two different processes, the RanGTPase cycle and sumoylation of specific targets (Fig. 5 B). Therefore, two distinct functions for RanGAP1 phosphorylation can be envisaged. RanGAP1 phosphorylation may modulate RanGAP1's catalytic activity. This modulation would have to involve recruitment of an unknown binding partner, as a direct effect of phosphorylation on the catalytic activity was not detected (Fig. S1, available at http://www.jcb.org/cgi/content/full/jcb.200309126/DC1). Alternatively, phosphorylated RanGAP1 may recruit specific SUMO target proteins to RanBP2's catalytic domain. Interestingly, RanBP2 has recently been found to be essential for kinetochore function in mitosis (Salina et al., 2003). Although it is not known if RanBP2 targets RanGAP1 to kinetochores (Joseph et al., 2002; Arnaoutov and Dasso, 2003), or if the E3 ligase activity is required at this site, sumoylation does have an important role in chromosome segregation (for review see Seeler and Dejean, 2003). Identification of binding partners for the mitotic RanGAP1*SUMO1–RanBP2 complex will aid in distinguishing between these predicted functions.

Materials and methods

Plasmids and recombinant proteins

The expression plasmid for mouse RanGAP1 was as described by Mahajan et al. (1997). Mutants of RanGAP1 were engineered by site-directed mutagenesis. Purification of recombinant RanGAP1 followed published procedures (Mahajan et al., 1997). In vitro sumoylation of RanGAP1 with Aos1/Uba2 and Ubc9 was as described by Pichler et al. (2002). Bacterially expressed p27 and cyclin A/Cdk2 expressed in baculovirus were prepared as described previously (Hengst et al., 1998; Hengst and Reed, 1996). Cyclin B/Cdk1 was purchased from Calbiochem.

Antibodies

Goat α-RanGAP1, goat α-Ubc9, rabbit α-RanBP2 (Pichler et al., 2002), and rabbit α–cyclin A antibodies were described previously (Hengst and Reed, 1996). For phosphospecific antibodies, the following peptides were coupled to ovalbumin: T409, CEKSApTPSRKI; S428, CPVLSpSPPPAD; and S442, CAFPpSPEKLLR. Initial injection into goats was as an emulsion with Titermax Gold (Sigma-Aldrich), booster injections were with Freund's incomplete adjuvant. Antibodies were affinity purified on phosphopeptides coupled to EAH-Sepharose 6B (Amersham Biosciences), eluted with 0.2 M acetic acid, pH 2.7, and 0.5 M NaCl, and dialyzed against PBS. Before use, antibodies were preadsorbed against immobilized nonphosphorylated peptides. Mouse α–cyclin B and rabbit α-GFP antibodies were obtained from Santa Cruz Biotechnology, Inc. Alexa 488 donkey α goat was purchased from Molecular Probes, other secondary antibodies were purchased from Jackson ImmunoResearch Laboratories.

Immunoblotting and fluorescence microscopy

Detection of antigens on nitrocellulose was performed with affinity-purified goat α p-T409 (0.5 μg/ml), α p-S428 (0.4 μg/ml), α p-S442 (0.7 μg/ml), or α RanGAP1 (0.25 μg/ml) in 5% milk powder (or 0.2% gelatine) in PBS, 0.2% Tween 20 for 1 h at RT. Detection was performed by chemiluminescence. For indirect immunofluorescence, adherent HeLa cells grown on coverslips were either fixed for 10 min with 2% PFA in PBS, 1 mM $MgCl_2$, and permeabilized for 5 min with 0.2% Triton X-100 in PBS, 1 mM $MgCl_2$, or permeabilized and fixed for 10 min in 4% PFA, 0.2% Triton X-100, 20 mM PIPES, 1 mM $MgCl_2$, and 10 mM EGTA (Kapoor et al., 2000). Antibodies in 2% BSA, PBS/$MgCl_2$ were used at 0.25 μg/ml

(α-RanGAP1), 1 μg/ml (α p-T409 and α p-S428), and 2 μg/ml (α p-S442), and at 1:100 (α cyclin B). Alexa 488 donkey α goat and Cy3 donkey α mouse antibodies were at 1:500. Hoechst 33342 was included with the secondary antibodies at 0.2 μg/ml. Pictures of cells mounted in ProLong Antifade (Molecular Probes) were taken with a microscope (model Axioskop II; Carl Zeiss MicroImaging, Inc.), 63× Plan Apochromat lens (aperture 1.4, oil), using a camera (model MicroMax CCD; Princeton Instruments) and Iplab software.

Immunoprecipitations

Immunoprecipitations were from SDS-lysates, digitonin cytosol, cytosol generated by hypotonic swelling, or from RIPA extracts from cycling and nocodazole-arrested HeLa cells. For SDS-lysate, HeLa suspension cells were lysed by boiling in 1% SDS and diluted 10-fold with RIPA buffer-SDS (50 mM Tris-HCl, pH 8, 150 mM NaCl, 1% NP-40, 0.5% deoxycholate, 1 mM DTT, and 1 μg/ml pepstatin, aprotinin, and leupeptin). Hypotonic swelling extracts were generated as described previously (Melchior, 1998), and buffer was changed to TB buffer with protease inhibitors and phosphatase inhibitor cocktail I (Sigma-Aldrich) using PD10 columns (Amersham Biosciences). For digitonin cytosol, HeLa cells were lysed in TB containing protease inhibitors and phosphatase inhibitor cocktail I and 0.005% digitonin (Calbiochem). For RIPA extracts, HeLa suspension cells were lysed by sonification in 4 vol RIPA buffer with protease inhibitors, phosphatase inhibitor cocktail I, and 10 mM iodoacetamide. All cell lysates were clarified at 100,000 *g* for 45 min before use in IP. Affinity-purified antibodies or control IgGs cross-linked at 2 mg/ml to Ultralink Immobilized Protein G Plus beads (Pierce Chemical Co.) were incubated with extracts for 90 min at 4°C. Beads were washed three times in RIPA buffer and boiled in SDS-Laemmli loading buffer.

Cell cycle analysis of RanGAP1 phosphorylation

A standard double thymidine block release protocol was used to obtain a synchronous population of suspension HeLa cells (Bonifacino et al., 1999). At indicated times, cells were harvested by centrifugation, aliquots flash frozen, and stored at −80°C. Aliquots were used for analysis by immunoblotting upon lysis in Laemmli buffer or for immunoprecipitation upon SDS-lysis. Progression through the cell cycle was monitored by FACS® analysis after cell fixation in 70% ethanol and staining with propidium iodide (Bonifacino et al., 1999). To determine the mitotic index, cells were fixed in 70% ethanol, stained using a final concentration of 4 ng/μl Hoechst 33342 (Molecular Probes), mounted with Glow mounting medium (EnerGene), and observed using a microscope (model Axioskop II; Carl Zeiss MicroImaging, Inc.).

In vitro RanGAP1 phosphorylation

Phosphorylation of 2 μg RanGAP1 with recombinant kinases was in 20 mM Tris-HCl, pH 7.5, 10 mM $MgCl_2$, 50 μM ATP, and 10 μCi γ[^{32}P]ATP at 30°C for 30 min. Cyclin B/Cdk1 (Calbiochem) and cyclin A/Cdk2 were used at 2 U or 5 ng, respectively. Analysis was performed by SDS-PAGE and autoradiography. Mitotic extracts for RanGAP1 phosphorylation were prepared from 100 ml of nocodazole-arrested HeLa cells by freeze-thaw lysis in 1.5 ml TB buffer supplemented with phosphatase inhibitor cocktail I. 100 ng of SUMO1-modified RanGAP1 was incubated in 5 μl of extracts and 1 mM of ATP at 30°C for 2 h. Recombinant p27 at concentrations of 1 μg or 5 μg was used to pretreat mitotic cell extracts on ice for 45 min. Reactions were analyzed by immunoblotting with α RanGAP1 antibodies.

Mass spectrometry

Coomassie-stained protein bands were in-gel digested by trypsin (sequencing grade; Promega) using essentially the protocol of Shevchenko et al. (1996) and desalted using home-made miniaturized reversed-phase columns (Gobom et al., 1999). MALDI-TOF mass spectra were acquired on a Reflex III instrument (Bruker Daltonik) in positive ion reflector mode. As a matrix, 2,5 dihydroxybenzoic acid (Bruker Daltonik) was used. For peptide sequence analysis by electrospray tandem mass spectrometry, samples were filled into nano electrospray needles (Protana) and analyzed on an ion trap (model Esquire 3000+; Bruker Daltonik) mass spectrometer.

Online supplemental material

GAP assays were performed as described previously (Mahajan et al., 1997) using α-[^{32}P]Ran-GTP and immunoprecipitated or using recombinant RanGAP1. Analysis was performed by TLC. Amounts of GTP and GDP were determined using a PhosphorImager (model BAS-2500, Fuji FILM). Online supplemental material is available at http://www.jcb.org/cgi/content/full/jcb.200309126/DC1.

We are grateful for many stimulating discussions with Dr. Andrea Pichler and other members of the laboratory. Dr. Frank Freudenmann is acknowledged for peptide synthesis and Dr. Heinz Brandtstetter for immunization services.

This work was funded by the Bundesministerium für Bildung und Forschung (grant BioFUTURE 0311869), an Alexander von Humboldt fellowship (to S. Swaminathan), and the Max-Planck Institute for Biochemistry.

Submitted: 22 September 2003
Accepted: 18 February 2004

References

Arnaoutov, A., and M. Dasso. 2003. The Ran GTPase regulates kinetochore function. *Dev. Cell.* 5:99–111.

Bonifacino, J.S., M. Dasso, J. Lippincott-Schwartz, J.B. Harford, and K.M. Yamada. 1999. Current Protocols in Cell Biology. John Wiley and Sons, New York. Also available at http://www.mrw2.interscience.wiley.com/cponline.

Favreau, C., H.J. Worman, R.W. Wozniak, T. Frappier, and J.C. Courvalin. 1996. Cell cycle-dependent phosphorylation of nucleoporins and nuclear pore membrane protein Gp210. *Biochemistry.* 35:8035–8044.

Gobom, J., E. Nordhoff, E. Mirgorodskaya, R. Ekman, and P. Roepstorff. 1999. Sample purification and preparation technique based on nano-scale reversed-phase columns for the sensitive analysis of complex peptide mixtures by matrix-assisted laser desorption/ionization mass spectrometry. *J. Mass Spectrom.* 34:105–116.

Guarguaglini, G., L. Renzi, F. D'Ottavio, B. Di Fiore, M. Casenghi, E. Cundari, and P. Lavia. 2000. Regulated Ran-binding protein 1 activity is required for organization and function of the mitotic spindle in mammalian cells in vivo. *Cell Growth Differ.* 11:455–465.

Hengst, L., and S.I. Reed. 1996. Translational control of p27Kip1 accumulation during the cell cycle. *Science.* 271:1861–1864.

Hengst, L., and S.I. Reed. 1998. Inhibitors of the Cip/Kip family. *Curr. Top. Microbiol. Immunol.* 227:25–41.

Hengst, L., U. Gopfert, H.A. Lashuel, and S.I. Reed. 1998. Complete inhibition of Cdk/cyclin by one molecule of p21(Cip1). *Genes Dev.* 12:3882–3888.

Joseph, J., S.H. Tan, T.S. Karpova, J.G. McNally, and M. Dasso. 2002. SUMO-1 targets RanGAP1 to kinetochores and mitotic spindles. *J. Cell Biol.* 156: 595–602.

Kapoor, T.M., T.U. Mayer, M.L. Coughlin, and T.J. Mitchison. 2000. Probing spindle assembly mechanisms with monastrol, a small molecule inhibitor of the mitotic kinesin, Eg5. *J. Cell Biol.* 150:975–988.

Kreegipuu, A., N. Blom, and S. Brunak. 1999. PhosphoBase, a database of phosphorylation sites: release 2.0. *Nucleic Acids Res.* 27:237–239.

Li, H.Y., D. Wirtz, and Y. Zheng. 2003. A mechanism of coupling RCC1 mobility to RanGTP production on the chromatin in vivo. *J. Cell Biol.* 160:635–644.

Macaulay, C., E. Meier, and D.J. Forbes. 1995. Differential mitotic phosphorylation of proteins of the nuclear pore complex. *J. Biol. Chem.* 270:254–262.

Mahajan, R., C. Delphin, T. Guan, L. Gerace, and F. Melchior. 1997. A small ubiquitin-related polypeptide involved in targeting RanGAP1 to nuclear pore complex protein RanBP2. *Cell.* 88:97–107.

Matunis, M.J., E. Coutavas, and G. Blobel. 1996. A novel ubiquitin-like modification modulates the partitioning of the Ran-GTPase–activating protein RanGAP1 between the cytosol and the nuclear pore complex. *J. Cell Biol.* 135:1457–1470.

Matunis, M.J., J. Wu, and G. Blobel. 1998. SUMO-1 modification and its role in targeting the Ran GTPase-activating protein, RanGAP1, to the nuclear pore complex. *J. Cell Biol.* 140:499–509.

Melchior, F. 1998. Nuclear protein import in a permeabilized cell assay. *Methods Mol. Biol.* 88:265–273.

Pichler, A., A. Gast, J.S. Seeler, A. Dejean, and F. Melchior. 2002. The nucleoporin RanBP2 has SUMO1 E3 ligase activity. *Cell.* 108:109–120.

Quimby, B.B., and M. Dasso. 2003. The small GTPase Ran: interpreting the signs. *Curr. Opin. Cell Biol.* 15:338–344.

Salina, D., P. Enarson, J.B. Rattner, and B. Burke. 2003. Nup358 integrates nuclear envelope breakdown with kinetochore assembly. *J. Cell Biol.* 162:991–1001.

Seeler, J.S., and A. Dejean. 2003. Nuclear and unclear functions of SUMO. *Nat. Rev. Mol. Cell Biol.* 4:690–699.

Shevchenko, A., M. Wilm, O. Vorm, and M. Mann. 1996. Mass spectrometric sequencing of proteins from silver-stained polyacrylamide gels. *Anal. Chem.* 68:850–858.

Takizawa, C.G., and D.O. Morgan. 2000. Control of mitosis by changes in the subcellular location of cyclin-B1-Cdk1 and Cdc25C. *Curr. Opin. Cell Biol.* 12:658–665.

Toyoshima-Morimoto, F., E. Taniguchi, N. Shinya, A. Iwamatsu, and E. Nishida. 2001. Polo-like kinase 1 phosphorylates cyclin B1 and targets it to the nucleus during prophase. *Nature.* 410:215–220.

Walther, T.C., P. Askjaer, M. Gentzel, A. Habermann, G. Griffiths, M. Wilm, I.W. Mattaj, and M. Hetzer. 2003. RanGTP mediates nuclear pore complex assembly. *Nature.* 424:689–694.

Yang, J., and S. Kornbluth. 1999. All aboard the cyclin train: subcellular trafficking of cyclins and their CDK partners. *Trends Cell Biol.* 9:207–210.

Zhang, H., H. Saitoh, and M.J. Matunis. 2002. Enzymes of the SUMO modification pathway localize to filaments of the nuclear pore complex. *Mol. Cell. Biol.* 22:6498–6508.